Numerical simulation of the interaction between suspended sediment and moving plate based on the drift-flux model

Bo Yang , Bingchen Liang, Qin Zhang

Ocean University of China

2020/12/10

Outline

1. Background
2. Numerical Model
3. Results and Discussion
   3.1 Settling of particles cloud
   3.2 Sediment bed/plate interaction
4. Conclusion

Background

- Three types of marine mineral deposits on the seafloor: Mn nodules, FeMn crusts and SMS deposits.

- Harvesting system activities and tailings discharge will make a large amount of sediment suspended in the water and cause irreversible impact on the marine environment.

- Sediment deposition and turbulent diffusion play an important role in the whole process.

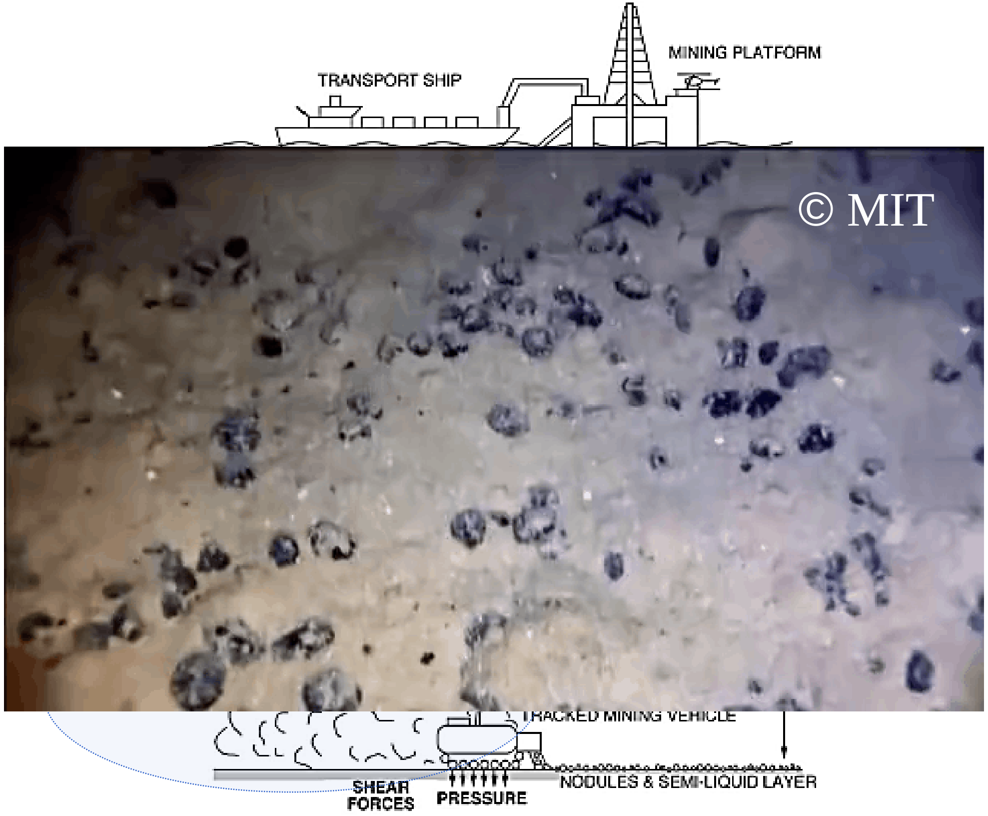

Fig 1. Deep-sea mining concept

Objectives

- ✓ Develop a CFD based two-phase mixture (drift-flux) model for turbulent diffusion and deposition of sediment laden flows.
- ✓ Understand the deposition and diffusion characteristics of disturbed sediment under different hydrodynamic conditions.
- ✓ Understand interaction between harvesting system and seabed to estimate and minimize seabed disturbance.

Research basis

- The two-phase mixture model was first proposed by Wallis (1969) and then further developed by Ishii (1975).
- Bertevas et al. (2019) further implanted it into the SPH method to simulate the turbulent sediment transport.

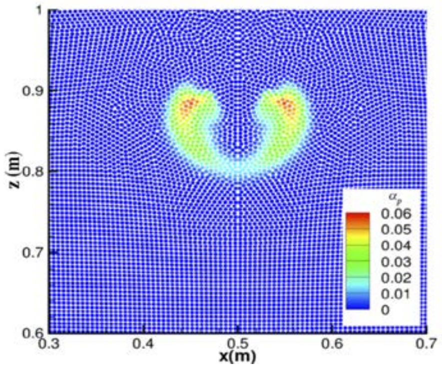

Fig 2. Settling of particles cloud (Bertevas et al. 2019)

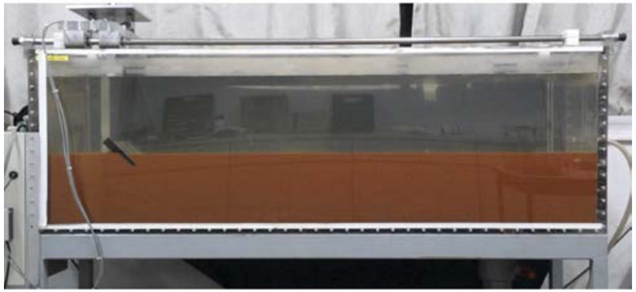

Fig 3. Experimental of the bentonite clay/water bed and translating inclined plate. (Bertevas et al. 2019)

Numerical Model

The Euler- Euler model continuity and momentum equations or each phase *i* as follows:

$$\frac{\partial \alpha_i \rho_i}{\partial t} + \nabla \bullet (\alpha_i \rho_i \mathbf{u}_i) = 0 \qquad (1)$$

$$\frac{\partial \alpha_i \rho_i \mathbf{u}_i}{\partial t} + \nabla \bullet (\alpha_i \rho_i \mathbf{u}_i \mathbf{u}_i) = -\alpha_i \nabla p_i + \nabla \bullet (\alpha_i (\boldsymbol{\tau} + \boldsymbol{\tau}_T)) + \alpha_i \rho_i \mathbf{g} + M_i \qquad (2)$$

The primary governing equations of the two-phase mixture (drift-flux) model are obtained by summing over all phases in Euler- Euler model, according to the following definition of the mixture.

$$\frac{\partial \rho_m}{\partial t} + \nabla \bullet (\rho_m \mathbf{u}_m) = 0 \qquad (3)$$

$$\frac{\partial \rho_m \mathbf{u}_m}{\partial t} + \nabla \bullet (\rho_m \mathbf{u}_m \mathbf{u}_m) = -\nabla p_m + \nabla \bullet (\boldsymbol{\tau} + \boldsymbol{\tau}_T - \boldsymbol{\tau}_{Dm}) + \rho_m \mathbf{g} + M_m \qquad (4)$$

$$\rho_m = \alpha_s \rho_s + \alpha_f \rho_f \quad (5) \qquad \mathbf{u}_m = \frac{\alpha_s \rho_s \mathbf{u}_s - \alpha_f \rho_f \mathbf{u}_f}{\rho_m} = c_s \mathbf{u}_s + c_f \mathbf{u}_f \quad (6) \qquad c_s = \frac{\alpha_s \rho_s}{\rho_m} \quad (7) \qquad c_f = (1 - c_s) = \frac{\alpha_f \rho_f}{\rho_m} \quad (8)$$

The phase pressures are often taken to be equal. $p_i = p_m$. The subscripts *s* and *f* represent the sediment phase and the fluid phase, respectively

Numerical Model

The three stress tensors $\boldsymbol{\tau}$, $\boldsymbol{\tau}_T$ and $\boldsymbol{\tau}_{\mathrm{Dm}}$ are represent the average viscous stress, turbulent stress and diffusion stress due to the phase slip:

$$\boldsymbol{\tau}_{Dm} = \alpha_s \rho_s \mathbf{u}_{sm} \mathbf{u}_{sm} + \alpha_f \rho_f \mathbf{u}_{fm} \mathbf{u}_{fm} \qquad (9)$$

The $\mathbf{u}_{sm}$ and $\mathbf{u}_{fm}$ are the diffusion velocities of each phase (the velocity with respect to the mass center of the mixture), are defined by:

$$\mathbf{u}_{sm} = \mathbf{u}_s - \mathbf{u}_m \quad (10) \qquad \mathbf{u}_{fm} = \mathbf{u}_f - \mathbf{u}_m \quad (11) \qquad \alpha_s \rho_s \mathbf{u}_{sm} + \alpha_f \rho_f \mathbf{u}_{fm} = 0 \quad (12)$$

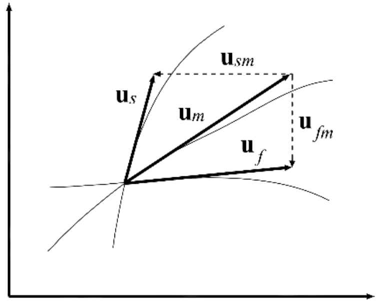

Fig 5. Definition of diffusion velocities.

In practice, the diffusion velocity has to be determined through the relative velocity which is defined as the velocity of the sediment phase relative to the velocity of the fluid phase:

$$\mathbf{u}_{sf} = \mathbf{u}_s - \mathbf{u}_f \qquad (13)$$

Then the diffusion velocity of sediment phase is given by:

$$\mathbf{u}_{sm} = (1 - c_s)\mathbf{u}_{sf} \qquad (14)$$

Numerical Model

For sand particle, a common form for the relative velocity (Manninen et al. 1996) :

$$\mathbf{u}_{sf0} = \frac{4d_s}{3C_D\left|\mathbf{u}_{sf0}\right|}\frac{\rho_s-\rho_m}{\rho_f}\left[\mathbf{g}-\frac{D\mathbf{u}_m}{Dt}\right] \quad (15)$$

The drag coefficient C_D is calculated by:

$$C_D = \frac{24}{\mathrm{Re}_s}\left(1+0.15\mathrm{Re}_s^{0.687}\right) \qquad \text{if } Re_s < 1000 \quad (16\text{ a})$$

$$C_D = 0.44 \qquad \text{if } Re_s \geq 1000 \quad (16\text{ b})$$

Re_s is the particle Reynolds number:

$$\mathrm{Re}_s = \frac{\left|\mathbf{u}_{sf0}\right| d_s}{\nu_f} \quad (17)$$

When the suspended sediment concentration is high, the hindering effect is considered:

$$\mathbf{u}_{sf} = \mathbf{u}_{sf0}(1-\alpha_s)^n \quad (18) \qquad n = \frac{4.7+0.41\mathrm{Re}_s^{0.75}}{1+0.175\mathrm{Re}_s^{0.75}} \quad (19)$$

For clay particles, the flocculation of sediment needs to be considered (Bertevas et al. 2019) :

$$\mathbf{u}_{sf0} = \frac{\alpha}{\beta}\frac{\rho_s-\rho_m}{18\mu_m} d_s^{3-n_f}\frac{d_{fc}^{n_f-1}}{1+0.15\mathrm{Re}_{fc}^{0.687}}\left[\mathbf{g}-\frac{D\mathbf{u}_m}{Dt}\right] \quad (20)$$

where $\alpha = \beta = 1$, $n_f = 2$, d_s and d_{fc} represent particle diameter and floc diameter, respectively. μ_m is the shear viscosity. Re_{fc} is the particle Reynolds number of floc.

$$\mathbf{u}_{sf} = \mathbf{u}_{sf0}\frac{(1-\alpha_{fc})^M(1-\alpha_s)}{1+2.5\alpha_{fc}} \quad (21)$$

where $\alpha_{fc} = \min(1.0, \alpha_d/\alpha_{gel})$, α_{gel} is the gelling fraction at which the flocs form a continuous network and $M = 2.0$ is chosen.

Numerical Model

The viscous stress and turbulent stress are defined as:

$$\boldsymbol{\tau} = 2\mu_m(\alpha_s)\mathbf{D} \quad (22)$$

$$\boldsymbol{\tau}_T = 2\mu_T\mathbf{D} - \frac{2k}{3}\mathbf{I} \quad (23)$$

where **I** is the identity matrix, and **D** is the strain-rate tensor:

$$\mathbf{D} = \frac{1}{2}[\nabla\mathbf{u}_m + (\nabla\mathbf{u}_m)^T] \quad (24)$$

The buoyancy modified k-omega SST model is used for turbulence closure:

$$\frac{D\rho_m k}{Dt} = \rho_m P_k + G_k - \rho_m\beta^* k\omega + \nabla\cdot(\rho_m(\nu + \sigma_k\nu_T)\nabla k) \quad (25)$$

$$\frac{D\rho_m\omega}{Dt} = \frac{\alpha\rho_m P_k + \gamma G_k}{\nu_T} - \rho_m\beta\omega + \nabla\cdot[\rho_m(\nu + \sigma_\omega\nu_T)\nabla\omega] + \rho_m\xi\nabla k\cdot\nabla\omega \quad (26)$$

$$G_k = -\frac{\nu_T}{\sigma_t}\mathbf{g}\bullet\nabla\rho \quad (27)$$

$$\gamma = C_{1\varepsilon}C_{3\varepsilon} - 1 \quad (28)$$

Table 1. k-Omega SST model parameters

β^*	α_1	α_2	β_1	β_2	σ_{k1}	σ_{k2}	$\sigma_{\omega 1}$	$\sigma_{\omega 2}$	$C_{1\varepsilon}$	$C_{3\varepsilon}$
0.09	5/9	0.44	3/40	0.0828	0.85	1.0	0.5	0.856	1.44	thah(u_v/u_h)

Numerical Model

The VOF method is used to simulate the diffusion and deposition process of sediment in water:

$$\frac{\partial \alpha_s}{\partial t} + \nabla \bullet (\alpha_s (\mathbf{u}_m + \mathbf{u}_{sm})) = \nabla \bullet (\frac{\nu_T}{\sigma_s} \nabla \alpha_s) \qquad (29)$$

where σ_s is turbulent Schmidt number, the value is 1.0 in this study.

The above equations are solved numerically using the open-source CFD toolbox OpenFOAM-v2006.

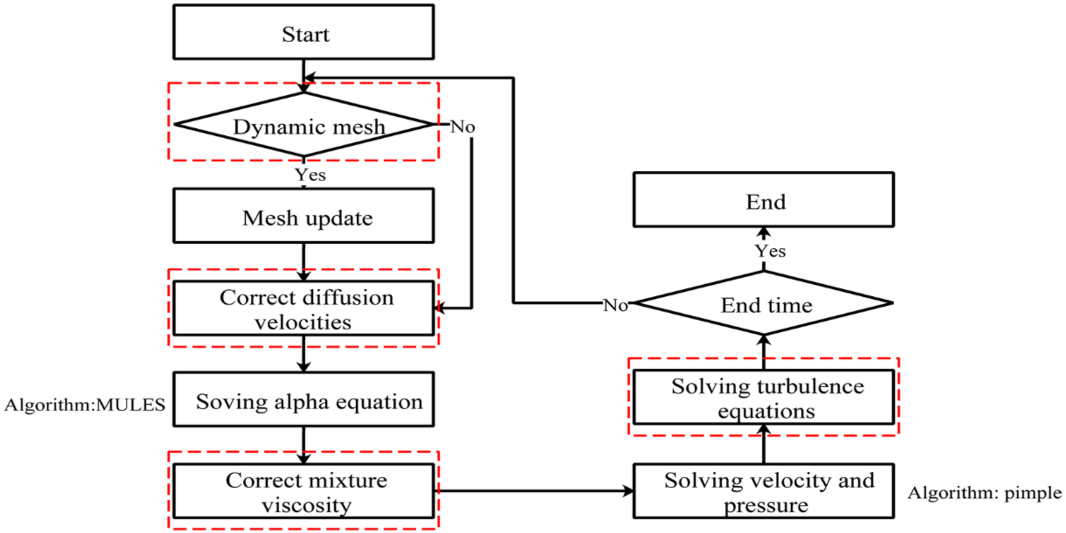

Fig. 6: Schematic for two-phase mixture CFD model.

Settling of particles cloud

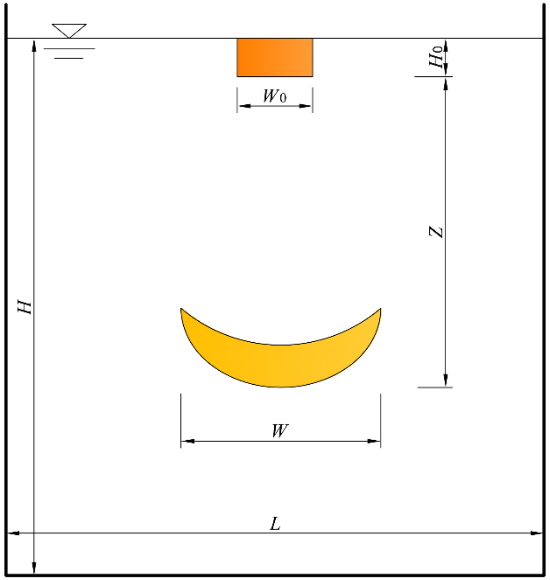

Fig 7. Sketch of particles dumping into a water tank

Table 2. Computational conditions of cases in Shi (2017)

Cases	***L*** **(m)**	***H*** **(m)**	H_0 **(cm)**	W_0 **(cm)**	q_0 **(cm^2)**	d_s **(mm)**	ρ_m **(kg/m^3)**	w_s **(cm/s)**
Case 1	1.0	1.0	2.5	2	5	0.8	2000	12.60
Case 3	1.0	1.0	2.5	2	5	5.0	2000	49.52
Case 5	1.0	1.0	2.5	4	10	1.3	2000	19.61
Case 6	1.0	1.0	2.5	4	10	5.0	2000	49.52

Suspension viscosity model (ahilan and Sleath, 1987):

$$\mu_m = \mu_f\left((1-\alpha_s) + 1.2\,\alpha_s \frac{\rho_f}{\rho_s}\left[\left(\frac{\alpha_{sMax}}{\alpha_s}\right)^{1/3} - 1\right]^{-2}\right) \qquad (30)$$

$$\alpha_{sMax} = 0.606$$

relative velocity :

$$\mathbf{u}_{sf0} = \frac{4d_s}{3C_D\left|\mathbf{u}_{sf0}\right|}\frac{\rho_s-\rho_m}{\rho_f}\mathbf{g} \qquad (31)$$

$$\mathbf{u}_{sf} = \mathbf{u}_{sf0}(1-\alpha_s)^{2.65} \qquad (32)$$

Settling of particles cloud

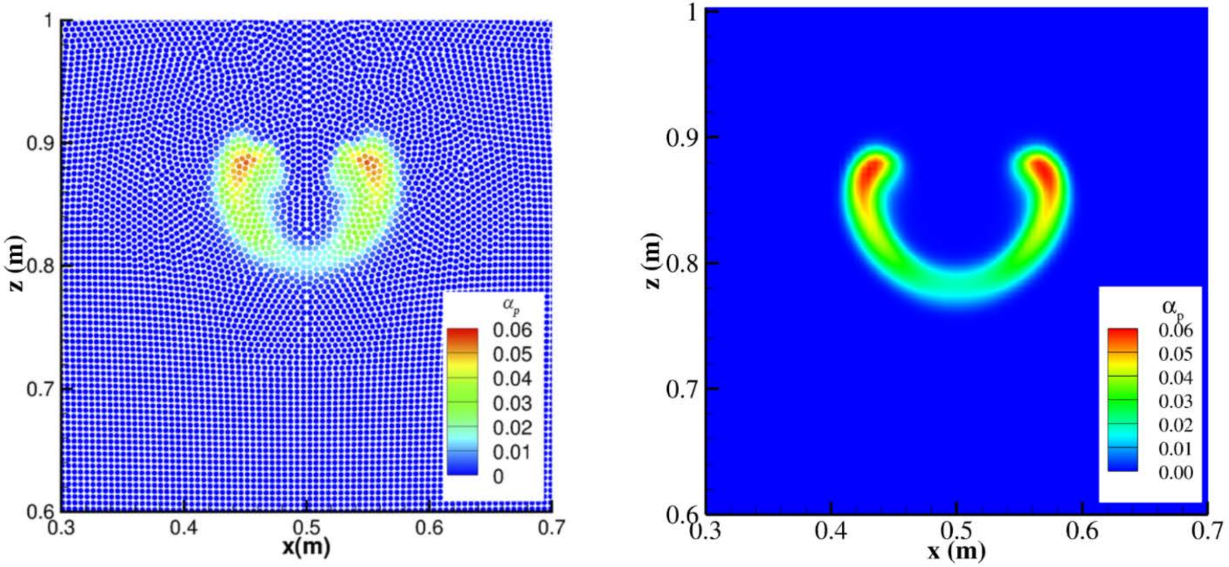

Fig 8. Comparison of volume fraction of the clouds between SPH (left) and CFD (right) model in case 1 at t = 1 s

Settling of particles cloud

$$U_0 = \sqrt{\frac{\rho_s - \rho_f}{\rho_f} L_0 g} \quad (33)$$

$$L_0 = \sqrt{q} \quad (34)$$

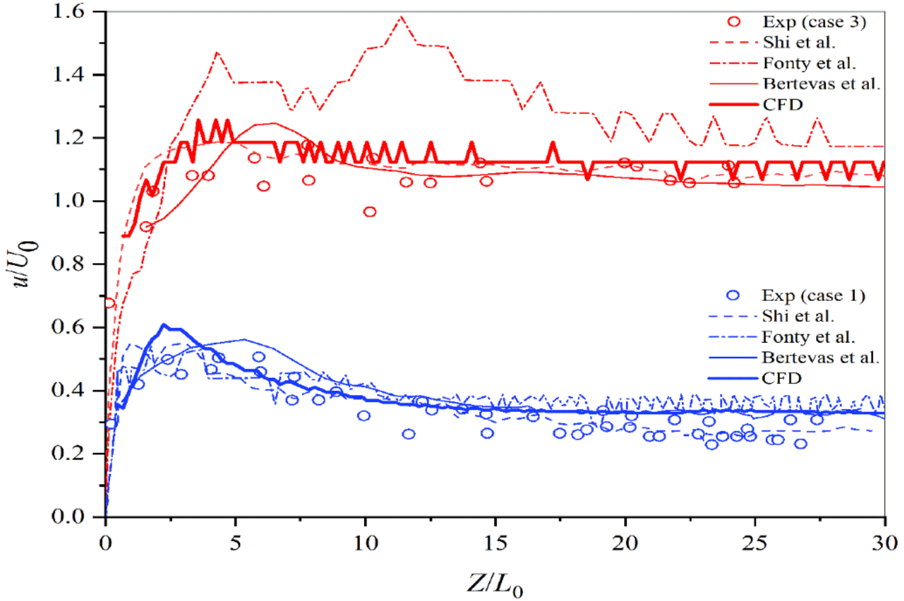

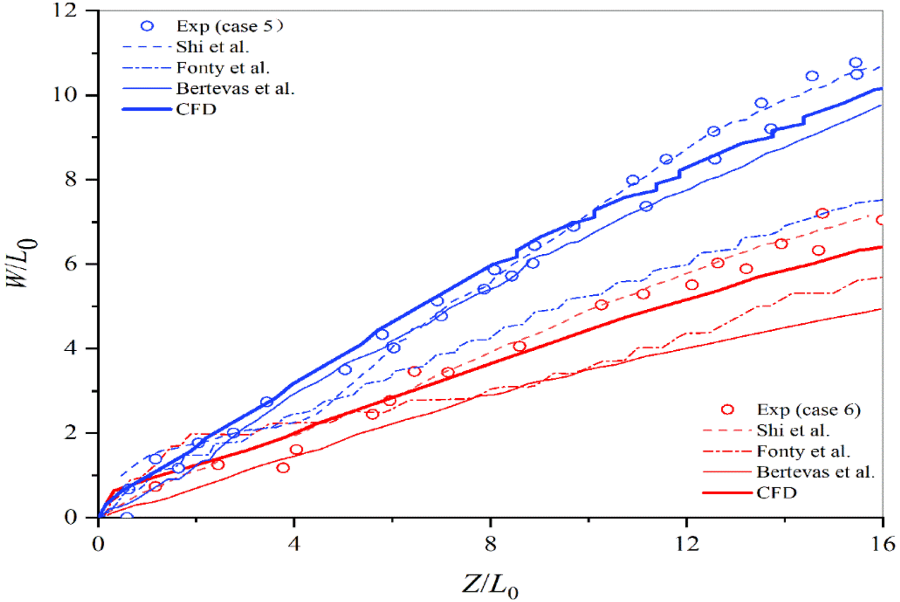

Fig 9. Evolution of the cloud front velocity (left) and cloud width (right). Comparison between the present results, the experimental of Nakatsuji et al. (1990) and the SPH simulation results of Shi et al. (2017) and Fonty et al. (2019) and Bertevas et al. (2019). Results for cases 1 (6) and 3 (5) are plotted in blue and red, respectively.

Sediment bed/plate interaction

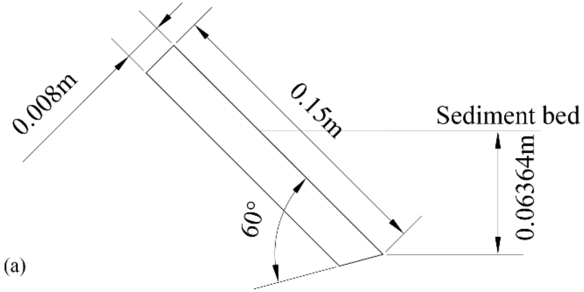

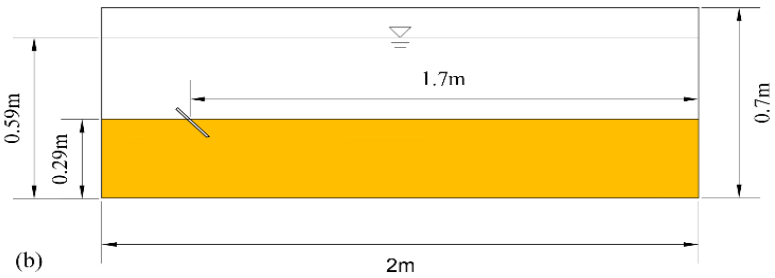

Fig. 10 (a) The geometric parameters of the plate. (b) The tank layout.

Table 3. Experiment\numerical simulation parameter setting

A (m/s^2)	V (m/s)	d_s (μm)	d_{fc} (μm)	ρ_s (kg/m^3)	α_s	α_{gel}
0.0282	0.142	4	200	2650	0.00768	0.02

Bingham-Papanastasiou model:

$$\mu_m = \mu^{\infty} + \frac{\tau_y}{\gamma_d}\left(1 - e^{-m\gamma_d}\right) \qquad (35)$$

$$\gamma_d = \sqrt{2\,\mathbf{D} : \mathbf{D}} \qquad (36)$$

where μ^{∞} is the high shear rate viscosity, τ_y is the yield stress, m is a parameter describing the yield stress growth at low shear rates

Sediment bed/plate interaction

Arbitrarily coupled mesh interface (ACMI) methods

- Mesh divided into the stationary zones and the moving zone.
- The moving zone move to the right with a given speed, the stationary zones remain stationary.
- The overlapping boundary is the ACMI boundary, and the non-overlapping boundary is the Wall boundary. Only ACMI boundary exists data interpolation and transfer between different regions.

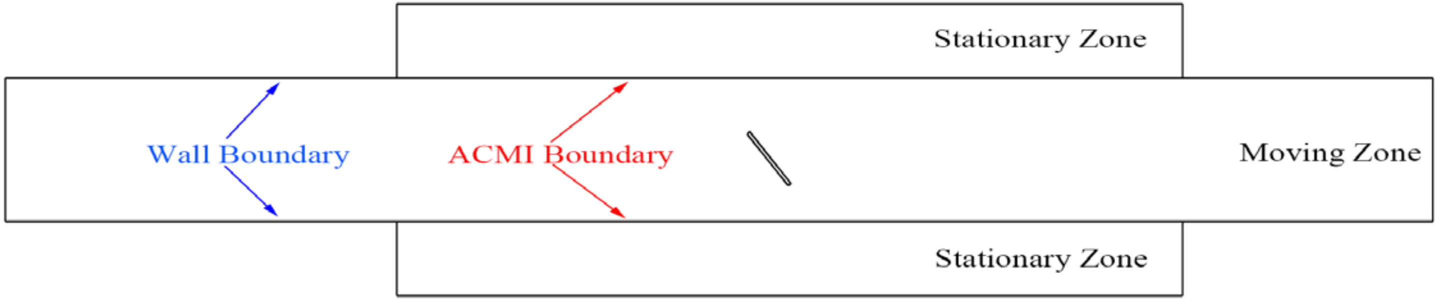

Fig. 11 ACMI mesh layout (t = 7 s after plate motion initiation).

Sediment bed/plate interaction

Arbitrarily coupled mesh interface (ACMI) methods

- Mesh divided into the stationary zones and the moving zone.
- The moving zone move to the right with a given speed, the stationary zones remain stationary.
- The overlapping boundary is the ACMI boundary, and the non-overlapping boundary is the Wall boundary. Only ACMI boundary exists data interpolation and transfer between different regions.

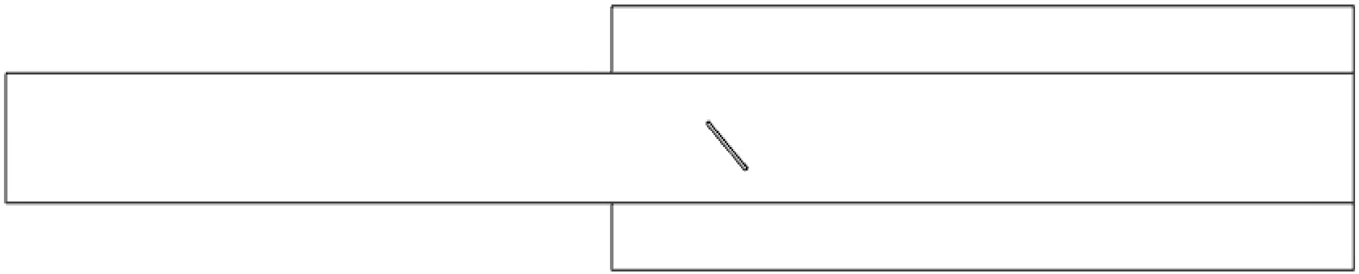

Fig. 12 ACMI mesh motion

Sediment bed/plate interaction

Arbitrarily coupled mesh interface (ACMI) methods

- Mesh divided into the stationary zones and the moving zone.
- The moving zone move to the right with a given speed, the stationary zones remain stationary.
- The overlapping boundary is the ACMI boundary, and the non-overlapping boundary is the Wall boundary. Only ACMI boundary exists data interpolation and transfer between different regions.

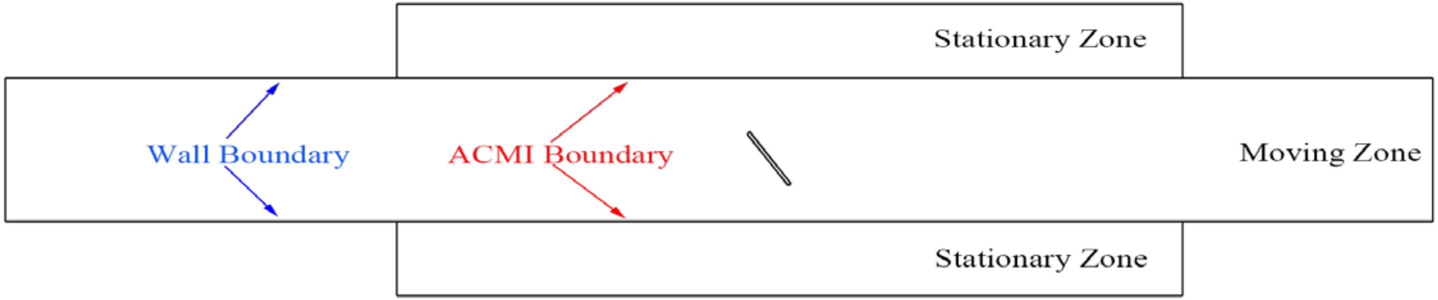

Fig. 11 ACMI mesh layout (t = 7 s after plate motion initiation).

Results and Discussion

Sediment bed/plate interaction

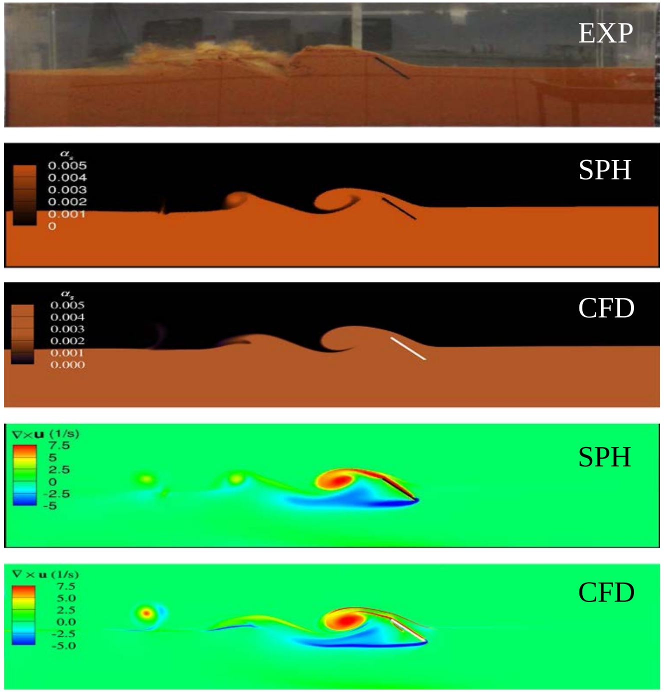

Fig. 13 Experimental (row 1), SPH simulation (Bertevas et al. 2019) and CFD simulation results shown at t = 9 s after plate motion initiation. SPH simulation results are for the sediment volume fraction (row 2), vorticity (row 4). CFD simulation results are for the sediment volume fraction (row 3), vorticity (row 5).

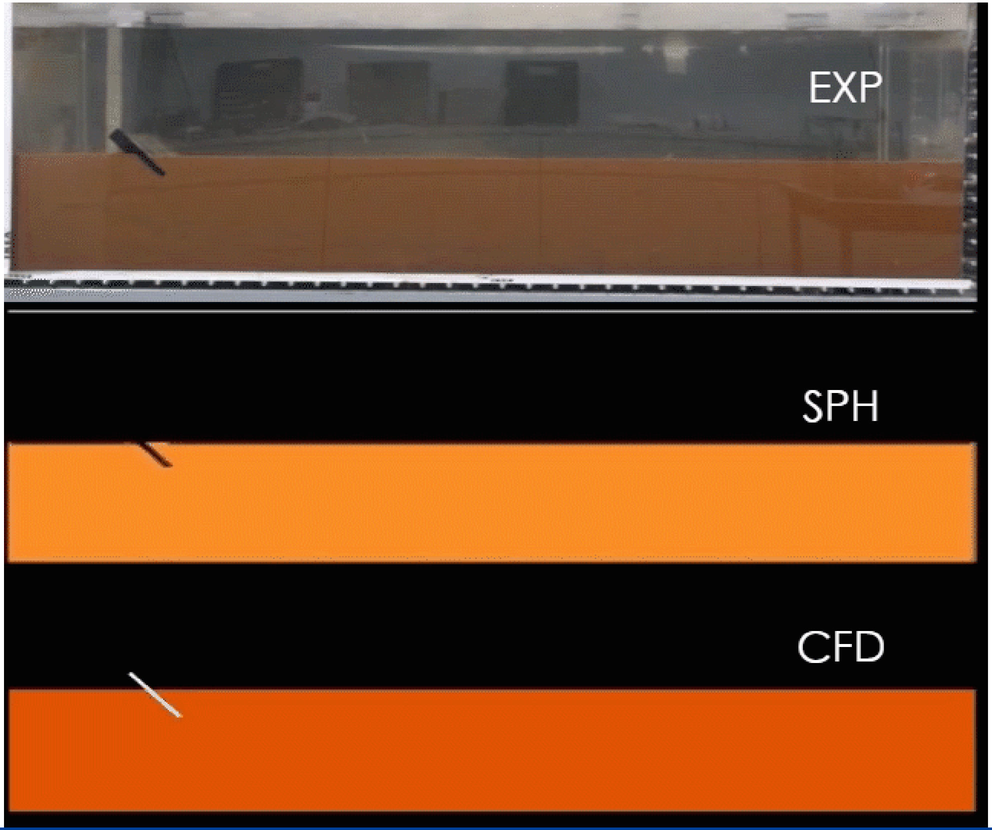

Sediment bed/plate interaction

Table 4. Mesh resolution setting

Meshes	**y_1 (mm)**	**Total number**
Mesh 1	1.25	268640
Mesh 2	1.00	465790
Mesh 4	0.85	675265
Mesh 3	0.75	821770

y_1 is the height of the first grid at the wall boundary of the plate.

Results and Discussion

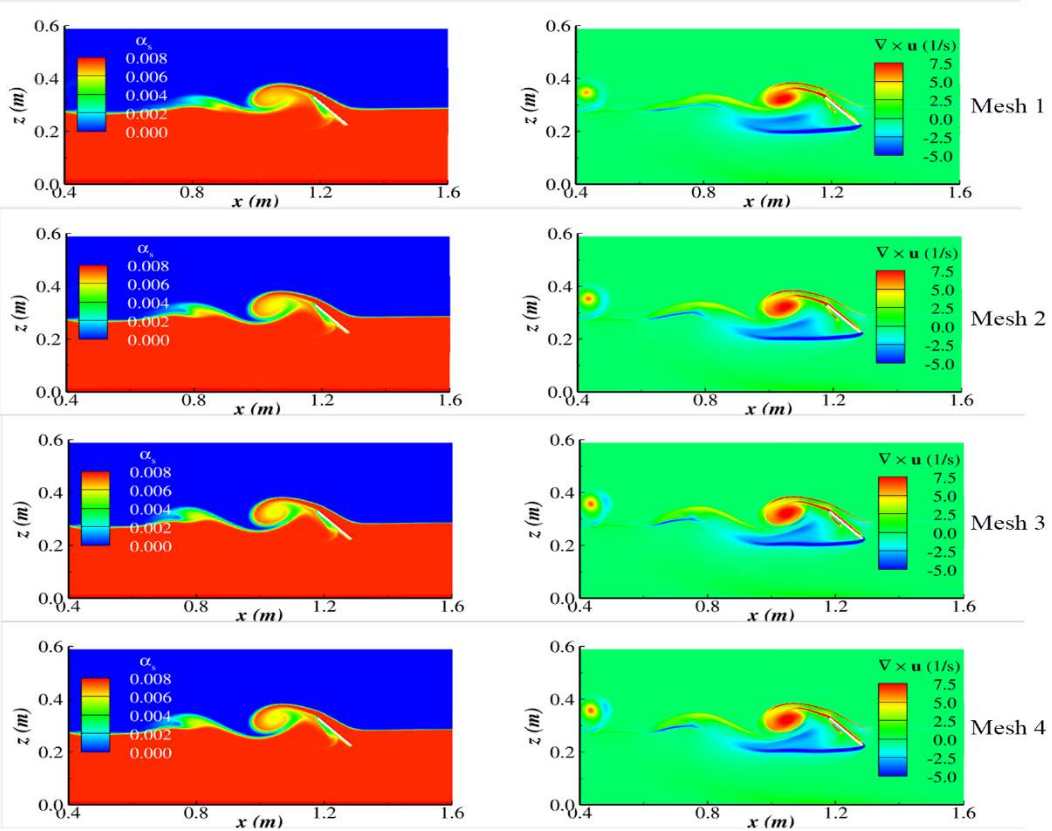

Fig. 14 Comparison of CFD simulation results at t = 9.0 s for four resolutions: Results are shown for the sediment volume fraction (column 1), vorticity (column 2)

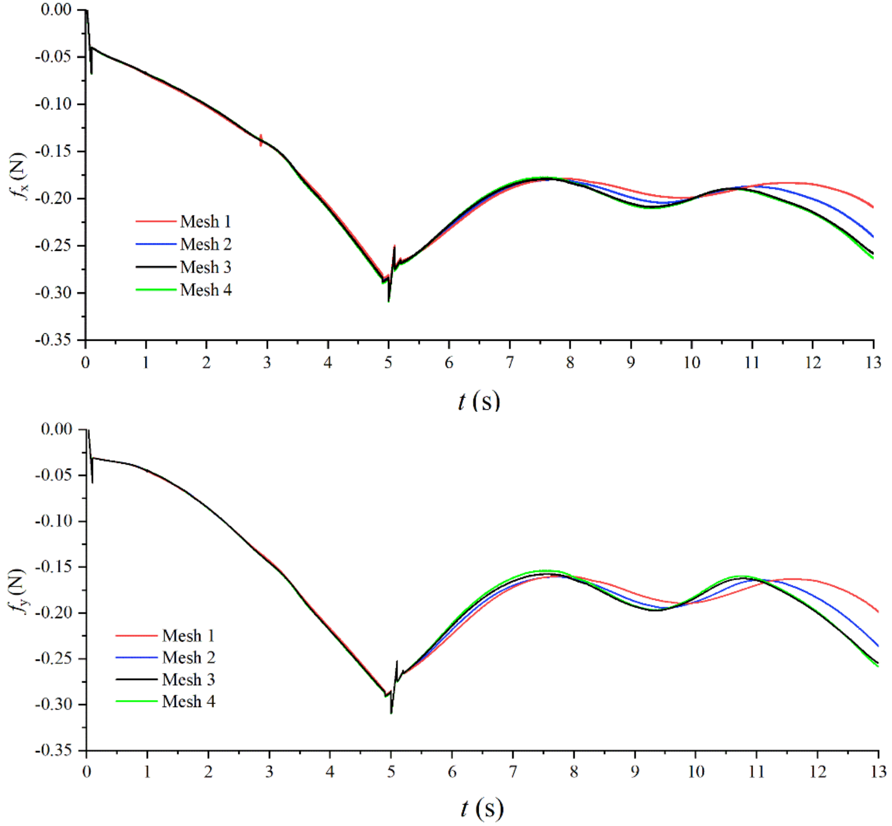

Fig. 15 The force comparison of the plate in the x (row 1) and y (row 2) directions at four resolutions

Results and Discussion

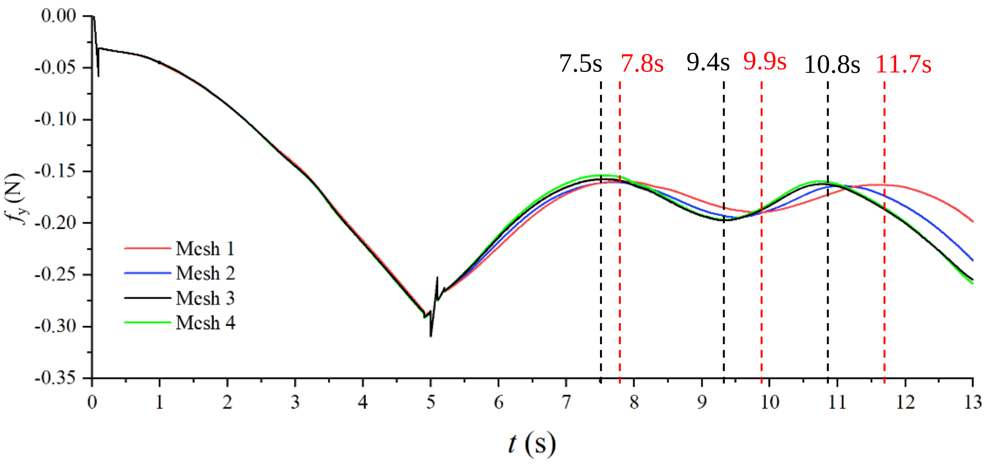

Fig 17. The force on the plate changes with time (Mesh 3)

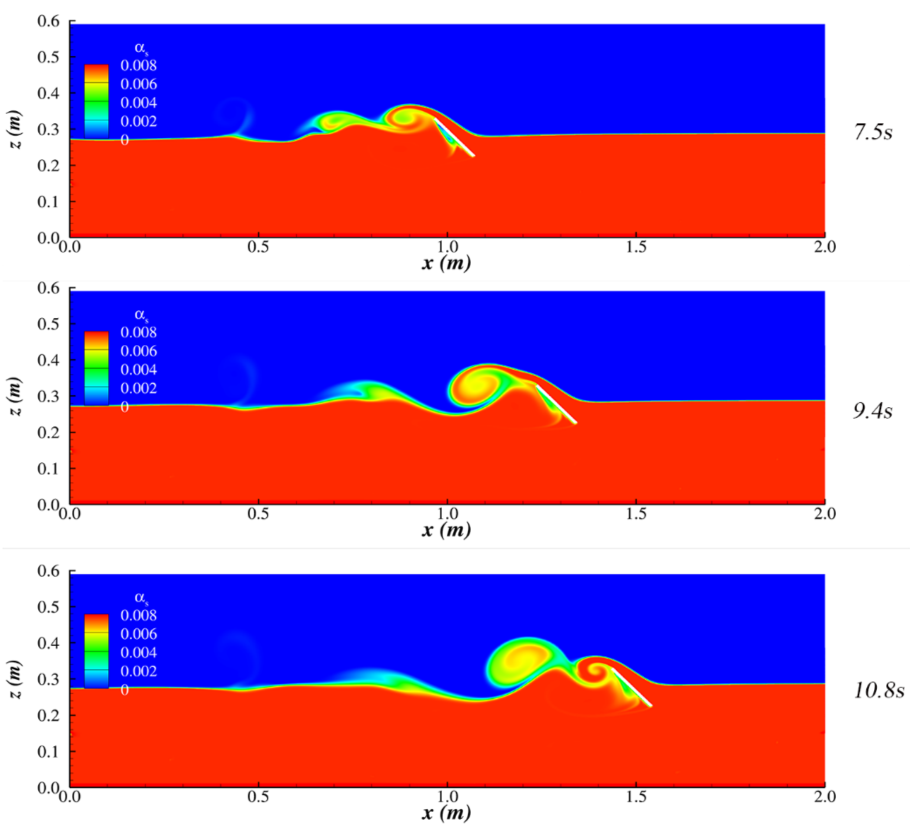

Fig 18. Sediment volume fraction at different times

Conclusion

- The two phase-mixture model based on CFD can achieve good results in simulating the process of sediment deposition and turbulent diffusion, especially considering the complexity of sediment movement.

- When the plate moves at a uniform speed, it will receive periodic force due to the shedding of the wake vortex.

- The mesh resolution has little effect on the simulation in the acceleration stage, but it has a great influence on the simulation in the uniform velocity stage, especially in the simulation of wake vortex shedding time and shedding position. And it has little effect on the force value on the plate.

- Under the actual sea conditions, the sediment diffusion process has strong three-dimensional characteristics. Therefore, further development of the three-dimensional model and three-dimensional DDES or LES simulation can more comprehensively capture the formation and development process of vortices.

Thanks for your attention!

Bo Yang
(+86) 15610053125
yangbo@stu.ouc.edu.cn